

Development of Automatically Controlled Cylindrical Coil Winding Machine

Mehmet Ermurat¹, Ömer Tutucu²

^{1,2}Department of Mechanical Engineering, Kahramanmaraş Sutcu Imam University
¹ermurat@ksu.edu.tr, ²omertutucu@gmail.com

Abstract

In this study, an automatic helical coil winding system was developed for cylindrical bobbins utilizing wires with circular cross-sections. The helical winding method was selected due to the compatibility of the wire's geometry with helical patterns and the minimal mechanical complexity it requires. To complement this approach, the linear winding technique was employed, as it offers the most appropriate strategy for coil fabrication when combined with helical winding.

A dedicated software was developed to operate the system, allowing users to input parameters such as turn number, wire diameter, and carcass width. Based on these inputs, the system automatically calculates the required winding parameters and executes the winding process. Furthermore, a step matrix algorithm was implemented to ensure the synchronized movement of the stepper motors, facilitating precise coordination between the rotational and translational axes.

Within the scope of the experimental work, coils were fabricated using wires of 0.2 mm, 0.45 mm, and 0.9 mm diameters, across various turn counts. The fabricated coils were subsequently evaluated based on their filling factor performance. The experimental findings demonstrated that larger wire diameters and higher turn counts generally yielded greater fill factor values, with a concurrent reduction in the deviation between theoretical calculations and experimental measurements. This outcome is primarily due to the superior dimensional stability and mechanical robustness of thicker wires during the winding process.

Keywords: Helical winding, Cylindrical coil, Automatic coil winding

1. INTRODUCTION

Coils are structures formed by winding a certain length of conductive wire, yarn, fiber, plastic, or similar materials onto a spool or reel. They are widely used across a broad range of industrial applications. For instance, yarn coils are utilized in textile manufacturing and handicraft knitting [1], while fiber coils find application in the production of fiberglass fabrics and carbon fiber tubes [2]. Coils made from plastic-based materials such as ABS, PLA, or PC are employed as raw materials in additive manufacturing technologies, especially in rapid prototyping systems [3]. Conductive wire coils, on the other hand, serve various functions in electric motors and electronic circuit components.

In coil manufacturing involving wires with circular cross-sections, coils are generally classified into four main categories based on their geometry: cylindrical coils, pancake (disk) coils, toroidal coils, and

windings defined as concentrated or distributed. Among these, cylindrical coils are the most commonly employed due to their versatility and wide range of applications compared to disk and toroidal configurations [4].

Various types and cross-sections of wires can be used in coil production. However, circular cross-section wires are commonly preferred owing to their practical advantages such as ease of handling, widespread material availability, and cost-effectiveness [4,5].

There are three primary winding patterns used for manufacturing cylindrical coils with circular cross-section wires: random winding, helical winding, and orthocyclic winding. The key factor distinguishing these winding types is the fill factor, defined as the ratio of the total cross-sectional area of the wound wires to the available cross-sectional area within the coil carcass. For random winding, the fill factor typically ranges between 65% and 75%; for helical winding, it ranges from 75% to 90.7%, whereas for orthocyclic winding, it reaches a maximum of 90.7%. Achieving this theoretical maximum fill factor requires special processing techniques [6]. As the fill factor increases, the complexity of the system mechanisms also increases, consequently leading to higher system costs.

Various winding techniques are employed in the production of coils using circular cross-section wires. The most common techniques include linear winding, flyer winding, needle winding, and toroidal core winding. Considering both system cost and structural complexity, the linear winding technique is more advantageous for producing cylindrical coils with helical winding compared to other winding methods [4].

Regardless of the coil carcass's shape—be it circular [7], square [8], rectangular, or any similar geometry—coils wound by placing wires side by side around a rotating axis are generally referred to as cylindrical coils. Representative illustrations of cylindrical coils with circular and square cross-sections are shown in Figure 1 [4].

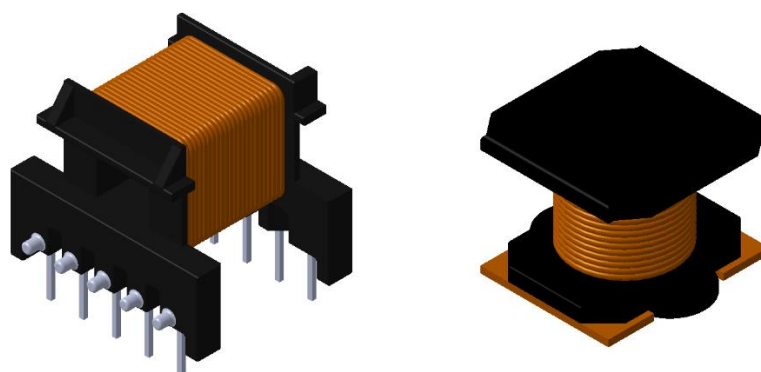


Figure 1. Rectangular and circular winding

Winding Patterns

To ensure efficient material usage and enhanced thermal management, coils must be designed as compactly as possible, provided that the necessary electrical and magnetic characteristics are maintained.

The ratio of the electrically conductive material (wire) to the available winding space in the coil is referred to as the mechanical fill factor [9].

Taking into account parameters such as the geometric characteristics of the planned coil carcass, the diameter of the conductor wire, and the number of turns, the fill factor can be calculated using Equation 1 [4]. A cross-sectional view of a wound sample coil is shown in Figure 2.

$$FF = \left[\frac{A * n}{(w * h)} \right] \quad (1)$$

Where FF is fill factor, A is wire conductor area, n is turn count, w is coil width and h is coil height.

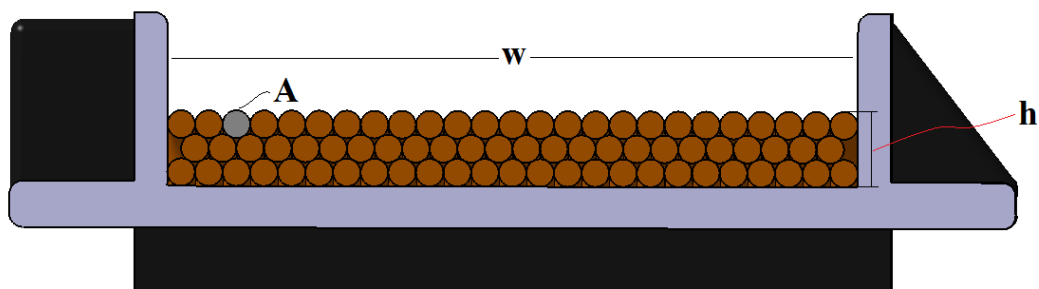


Figure **Error! No text of specified style in document.** Cross-sectional image of a sample coil after winding

Because air gaps are unavoidable in coils wound with circular wires, the fill factor is always less than one [9]. Minimizing air spaces in densely wound coils improves material efficiency and enhances thermal conductivity by allowing better heat dissipation from the current-carrying conductor wire, thereby improving device performance.

Three common winding patterns are used with circular wires: random winding, orthocyclic winding, and helical winding, each with distinct structural characteristics and fill factors.

Random Winding

Also known as loose or chaotic winding, this technique results in a relatively low fill factor. The irregular placement of the wire leads to non-uniform spacing, requiring a longer wire for the same number of turns compared to more compact methods. This increases internal resistance and material consumption. Typical fill factors for random winding range between 65% and 75% [6].

Orthocyclic Winding

This pattern achieves the highest fill factor possible for circular wires [6]. In orthocyclic winding, each wire turn in the current layer fits into the spaces formed by the wires in the previous layer. Optimal packing is achieved when the wires are placed parallel to the coil flange. Each new turn is offset laterally by exactly one wire diameter (winding pitch). In a properly executed orthocyclic winding, the imaginary lines connecting wire centers form equilateral triangles, as shown in Figure 3. If the winding pitch is not maintained accurately, the wire's natural self-aligning behavior is disrupted, causing a transition to random winding.

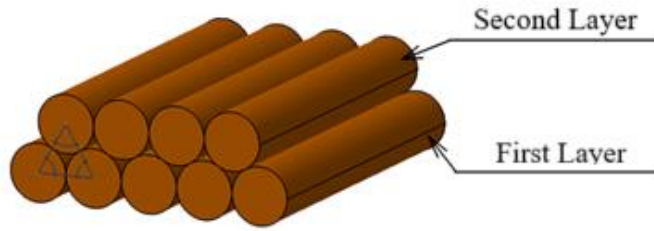


Figure 3. Equilateral triangle formed at the wire center in orthocyclic winding

Helical Winding

Helical winding features a screw-like structure within each winding layer, with a continuous and uninterrupted feed. Unlike orthocyclic winding, the layers are not parallel to the coil flange. However, within each layer, the winding pitch remains constant and equal to the wire diameter. In subsequent layers, wires may either rest atop the wires below or nest in the gaps between them. While the fill factor is lower than that of orthocyclic winding, it is still higher than random winding [4].

The winding direction alternates with each layer—e.g., clockwise followed by counterclockwise—resulting in a mixed stacking pattern where wires overlap twice and nest in gaps twice per turn. Figure 4 shows vertical and horizontal cross-sectional views of a helically wound coil, with Section A showing direct stacking and Section B highlighting nesting behavior.

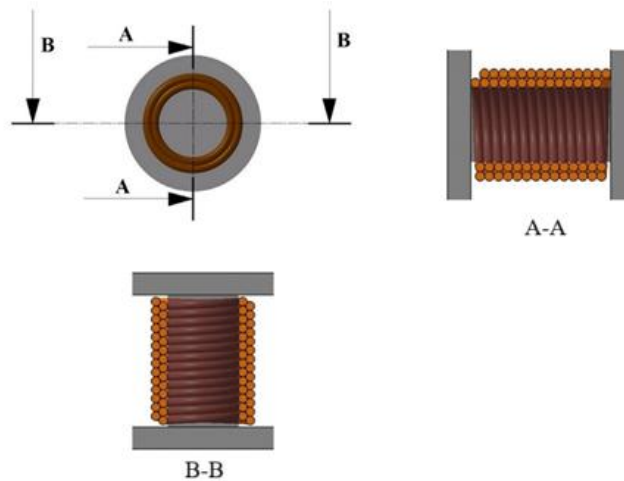


Figure 4. Helical coil from the vertical and horizontal cross-sectional areas

Since the stacking pattern varies throughout the coil, the winding height is not uniform. For helical winding, this height is calculated as the average of the heights associated with random and orthocyclic windings, as expressed in Equations 2.

$$h = \left[\left[\frac{(n * d^2) * (1 + \sin(60))}{2 * w} \right] + \frac{d}{2} \right]$$

(Error! No text of specified style in document.)

Where h is winding height, d is conductor diameter, n is winding count, and w is winding width.

Linear Winding Technique

The winding process is typically executed using the linear winding technique, where either the wire guide or the spool moves laterally to ensure uniform wire placement and a well-structured coil [10]. A schematic representation of this technique is provided in Figure 5.

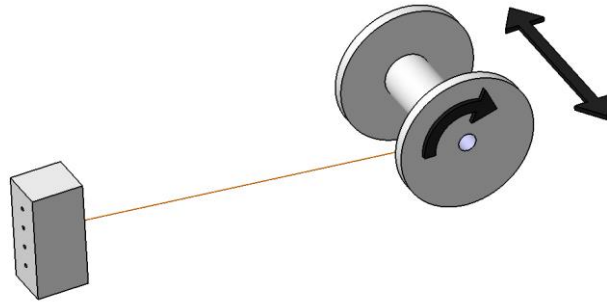


Figure 5. Linear winding

Considering its lower system complexity and cost compared to alternatives such as flyer or needle winding, the linear winding method is particularly suitable for producing helically wound cylindrical coils using circular cross-section wires.

Scope of This Study

In this study, a device based on the linear winding method was developed for the production of helically wound cylindrical coils using circular wires. The system is tailored for small- and medium-scale coil manufacturers and R&D institutions engaged in prototype fabrication. It aims to provide a practical, cost-efficient, and accessible solution for high-quality coil production.

2. EXPERIMENTAL SETUP

This section details the development and configuration of the automatic cylindrical coil winding system, designed for producing helical wound coils using wires with circular cross-sections and linear translation techniques. The system targets small- and medium-scale coil manufacturers as well as R&D laboratories engaged in prototype production.

The system consists of three principal components: the mechanical structure, the electronic system, and the control software. A CAD-rendered solid model of the system is provided in Figure 6.

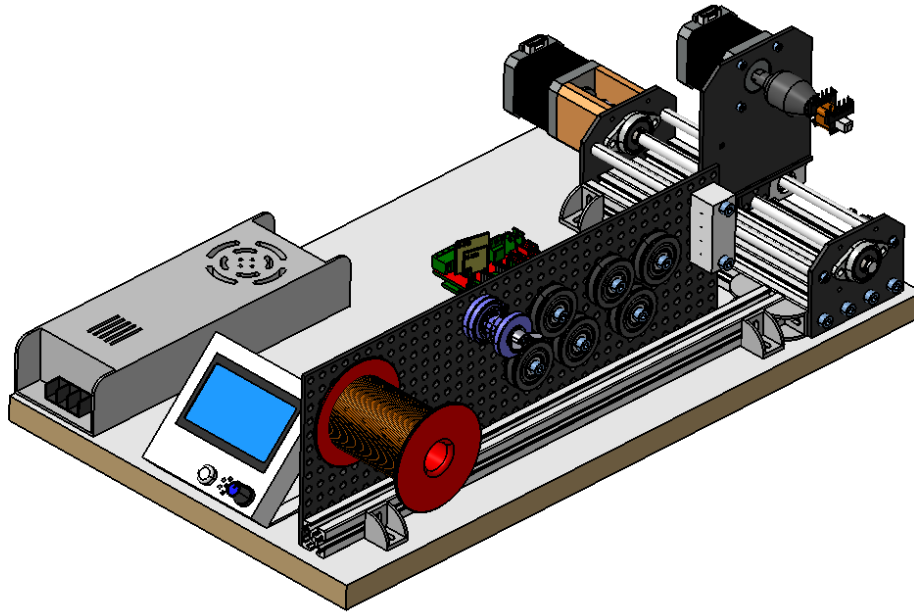


Figure 6. General view of the automatic coil winding system

Mechanical Structure

The mechanical structure integrates a linear drive system, a coil rotation mechanism, and a wire feeding unit. The linear drive system facilitates translational motion along two support shafts, powered by a lead screw connected to a stepper motor. The lead screw's rotary motion is translated into linear displacement via a lead screw nut, enabling the coil-holding carriage to move precisely along the support shafts.

The coil rotation mechanism secures the coil carcass and rotates it using an independent stepper motor, ensuring accurate wire deposition onto the coil body. Meanwhile, the wire feeding system—comprising a tension control mechanism, V-pulleys, and a Delrin guiding block—provides tensioned and straightened wire delivery during the winding process.

Electronic System

The electronic architecture of the system, illustrated in Figure 7, includes multiple stepper motors, motor drivers, limit switches, and an LCD interface, all orchestrated by an Arduino Mega 2560 microcontroller. A RAMPS 1.4 shield facilitates the integration of components and provides electrical protection [11, 12].

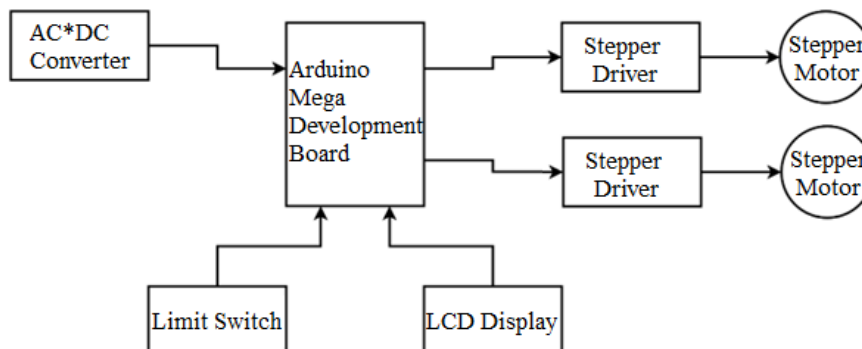


Figure 1. Electronic system components

The rotational and translational stepper motors are operated in precise synchronization through microcontroller-based software coordination [13,14]. This setup enables high-accuracy winding and allows independent or coupled control of system components as needed.

Software

The control software, developed in C++ using the Arduino IDE [15], governs the interaction between the electrical and mechanical components. It synchronizes coil rotation and wire translation, dynamically compensating for wire diameter variations using a "step matrix" strategy.

Essential parameters—including the number of coil layers, turns per layer, total coil height, and carcass positioning—are calculated automatically. An intuitive LCD-based user interface facilitates standalone operation, enabling operators to input winding parameters and monitor real-time system status.

Synchronous Motion

Precise synchronization between the translational and rotational movements is critical for achieving adjacent wire placement without gaps or overlaps, which directly affect the fill factor and coil structural integrity. Synchronization depends on the length of the coil carcass, wire cross-section, number of layers, and the number of wires per layer. Misalignment between the rotational and translational motors can lead to wire gaps or stacking. Microstep-level synchronization is ensured by implementing a step matrix algorithm [16].

The linear motion part of the system achieves a translational step size of approximately 6.25 $\mu\text{m}/\text{step}$ (160 steps/mm with a 1.25 mm lead screw). The rotational motion of the system requires 3200 microsteps for a full revolution, using 16-microstep motor drivers. Synchronous motion is achieved by coordinating microstep segments for both systems.

Step Matrix

Due to the sequential execution nature of microcontroller code, simultaneous rotational and translational movements are not inherently feasible. To address this, the step matrix divides each motion into microstep segments, which are then executed in parallel.

In this system, 3200 microsteps are needed for one full rotation and 2560 microsteps for 1 mm linear displacement. Since a linear or rotational movement cannot proceed unless the previous command is completed—due to the sequential execution nature of microcontroller code—true synchronous motion cannot be achieved by executing these commands consecutively. To enable synchronous movement, the rotational and translational motions are divided into smaller segments and controlled by corresponding instructions in the software. The microcontroller does not execute the next instruction until the current one is completed, so these segmented instructions ensure simultaneous execution.

Figure 8 presents a table of microstep sequences and repetition multipliers for wire diameters ranging from 0.05 mm to 1 mm. As the number of microsteps for rotation and translation depends on the wire diameter, the motors utilize the predefined microstep matrix to determine the correct number of steps to take for each wire diameter. This ensures synchronized motion throughout the winding process. Figure 9 compares the winding performance of 1 mm diameter wire using microstep control via the step matrix and conventional step control.

Total Rotation (turn)	Total Linear Motion (mm)	Step Motor Micro Step Sequence																Sequence Repeat Count
		Turn	Linear	Turn	Linear	Turn	Linear	Turn	Linear	Turn	Linear	Turn	Linear	Turn	Linear	Turn	Linear	
1	0,05	3	0	4	0	3	0	3	0	3	0	3	0	3	0	3	1	128
1	0,10	3	0	4	0	3	1	3	0	3	0	3	0	3	0	3	1	128
1	0,15	3	0	4	1	3	0	3	1	3	0	3	1	3	0	3	0	128
1	0,20	3	0	4	1	3	0	3	1	3	0	3	1	3	0	3	1	128
1	0,25	5	1	5	1	5	1	5	1	5	1	5	1	5	1	5	1	80
1	0,30	3	1	4	1	3	0	3	1	3	1	3	1	3	1	3	0	128
1	0,35	3	1	4	1	3	1	3	1	3	1	3	1	3	1	3	0	128
1	0,40	3	1	4	1	3	1	3	1	3	1	3	1	3	1	3	1	128
1	0,45	3	2	4	1	3	1	3	1	3	1	3	1	3	1	3	1	128
1	0,50	5	2	5	2	5	2	5	2	5	2	5	2	5	2	5	2	80
1	0,55	3	2	4	2	3	2	3	1	3	1	3	1	3	1	3	1	128
1	0,60	3	2	4	2	3	2	3	2	3	1	3	1	3	1	3	1	128
1	0,65	3	2	4	2	3	2	3	2	3	2	3	1	3	1	3	1	128
1	0,70	3	2	4	2	3	2	3	2	3	2	3	2	3	1	3	1	128
1	0,75	5	3	5	3	5	3	5	3	5	3	5	3	5	3	5	3	80
1	0,80	3	2	4	2	3	2	3	2	3	2	3	2	3	2	3	2	128
1	0,85	3	3	4	2	3	2	3	2	3	2	3	2	3	2	3	2	128
1	0,90	3	3	4	3	3	2	3	2	3	2	3	2	3	2	3	2	128
1	0,95	3	3	4	3	3	3	3	2	3	2	3	2	3	2	3	2	128
1	1,00	5	4	5	4	5	4	5	4	5	4	5	4	5	4	5	4	80

Figure 8. Step motor micro-step matrix

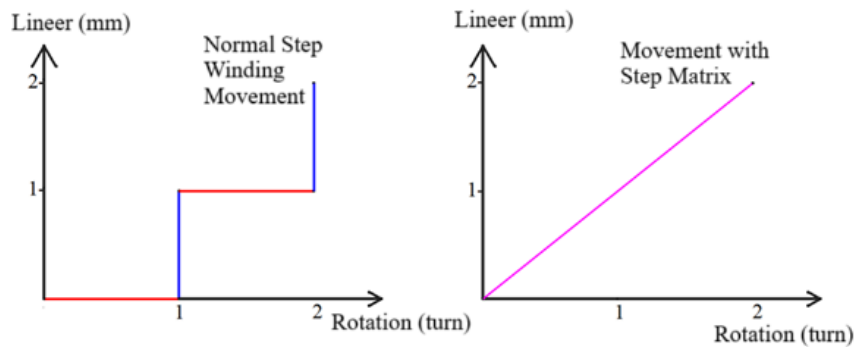


Figure 9. Comparison of step matrix micro-step and normal step winding motion

Prior to the winding operation, users input key parameters—coil length, wire diameter, and total turns—via the system interface. The software computes derived values such as layers, turns per layer, and total winding height.

Once the basic parameters have been entered and initiated “start winding” command by user, the microcontroller computes the corresponding winding parameters and generates the appropriate control commands to drive the stepper motors accordingly.

The system performs real-time monitoring and automatic adjustment to ensure consistent layers and whole winding process completion. Upon completion, the linear carriage resets for the next operation. A block diagram of this functional sequence is illustrated in Figure 10.

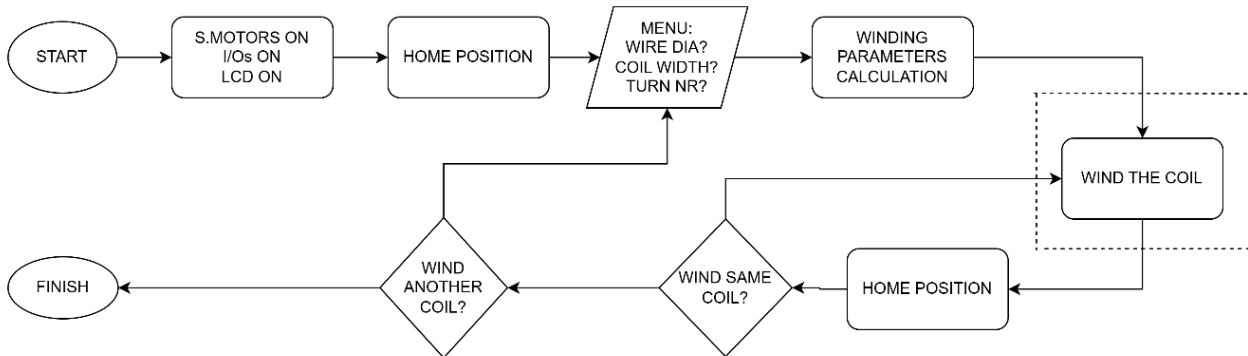


Figure 10. Block diagram of the coil winding process

Winding Functions

Self-Guiding Behavior in Layer Formation

During winding, wires exhibit a self-guiding behavior, aligning naturally beside each other when no external disturbance is present. To preserve this behavior and avoid gaps, the winding angle is applied in the opposite direction of coil rotation (Figure 11). This geometrical correction is handled algorithmically within the software.

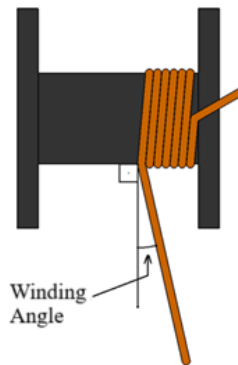


Figure 11. Winding angle

Layer Winding Mechanism

Precise coordination is required for each layer to contain the correct number of turns and maintain gap-free winding. The rotation mechanism completes one full revolution per turn, while the linear system advances by a distance equal to the wire diameter. This synchronous movement is achieved using the step matrix. Figure 12 presents the flow diagram of this layered winding operation.

System Interface

A dedicated LCD-based graphical interface enables standalone system operation. The interface allows for parameter input, real-time monitoring, and operational control via a multifunction rotary encoder button. On power-up, the main menu is displayed (Figure 13-a). Users can select submenus such as winding height

(Figure 13-b), start operation (Figure 13-c), and monitor the process in real time. The calculated winding height is automatically displayed to help the operator verify spatial feasibility on the coil core.

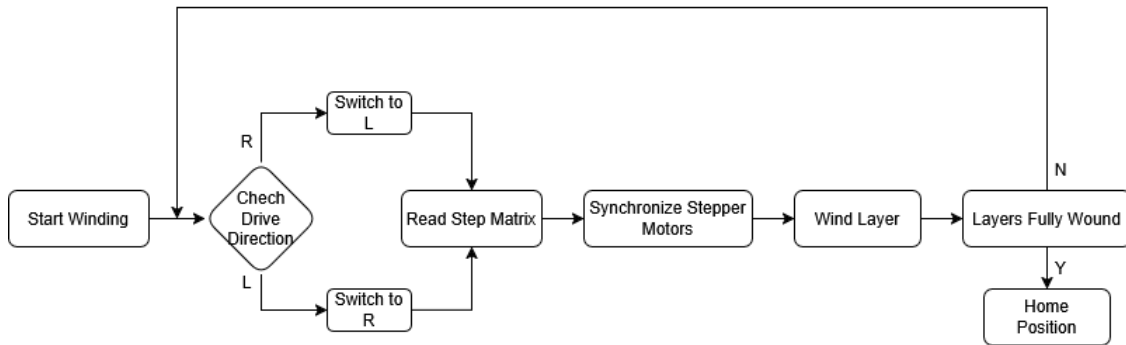


Figure 12. Block diagram of the layer winding process

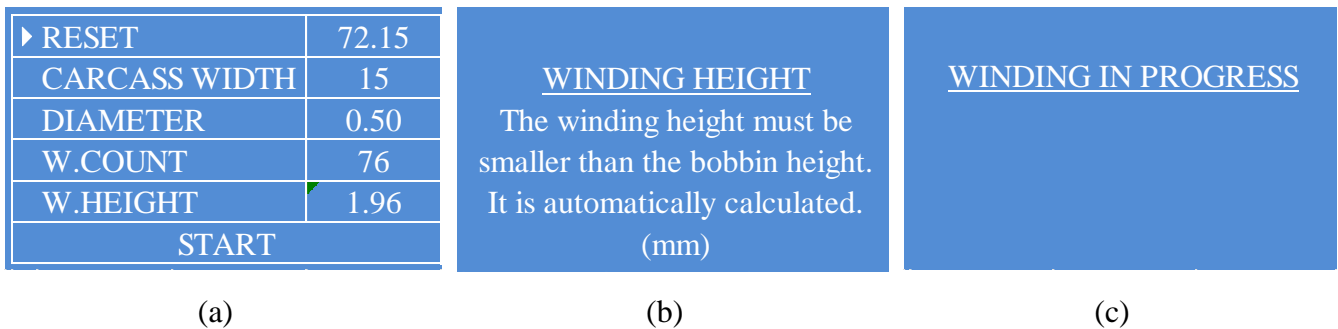


Figure 13. a) Main screen of the interface b) Winding height information screen c) Winding process information screen

3. EXAMINATION OF THE WOUND SAMPLE COILS

This section presents the examination of the sample coils wound by using the developed automatic cylindrical coil winding system.

Coils were produced by winding different numbers of turns using various wire diameters onto a single carcass. The wire diameter, number of turns, and carcass dimensions were selected randomly to evaluate the system's general applicability and robustness. The wound coil dimensions and fill factors were compared to theoretical values calculated via pre-defined geometric and analytical formulations. Based on this comparison, the system's average error rate was determined.

Prior to the winding process, the initial dimensions of the carcass—denoted as a , b , and w in Figure 14—were measured using a caliper to establish a reference for calculating the winding height and theoretical fill factor. After winding, the corresponding dimensions a' , b' , and w' were measured again using the same device, as shown in Figures 15 and 16, respectively.

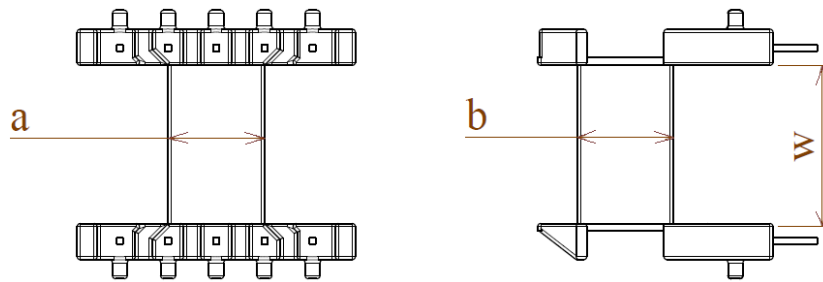


Figure 14. Carcass dimensions



(a)



(b)

Figure 15. Measuring the coil a' and b' dimensions



Figure 16. Coil w' dimension

Three different wire diameters—0.20 mm, 0.45 mm, and 0.90 mm—were tested to assess the system's ability to handle a range of wire sizes. For the 0.20 mm wire, 360, 300, 240, 180 and 120 turns were wound. For the 0.45 mm wire, 133, 106, 80, and 53 turns were applied, and for the 0.90 mm wire, 66, 53, 40, and 26 turns were wound.

The theoretical winding height for each sample was calculated using Equation 2, which accounts for the number of turns, wire diameter, and number of layers. The theoretical fill factor was computed according to Equation 1.

The implemented step matrix algorithm successfully maintained synchronous motion between the rotational and linear axes. Winding height measurements, which were used to determine the real fill factors, confirmed a deviation of less than $\pm 5\%$ between theoretical and actual values across all samples, particularly for wires ≥ 0.45 mm. The consistent winding heights and minimized stacking overlaps reflect a robust control over motion synchronization, confirming that the $6.25 \mu\text{m}/\text{step}$ linear resolution is suitable for sub-millimeter wire management.

Table 1 presents both the theoretical and measured values of fill factor for all samples. The percentage error between the theoretical and actual fill factors was then calculated.

Table 1. Wound coil results

Winding Nr.	Wire Diameter	Turn Count	Fill Factor (%) (Theoretical Results)	Fill Factor (%) (Measured Results)	Error (%)
Coil-1	0,2	120	84,18	72,22	14
Coil-2	0,2	180	86,24	74,80	13
Coil-3	0,2	240	87,31	75,70	13
Coil-4	0,2	300	87,97	75,88	14
Coil-5	0,2	360	88,41	77,41	12
Coil-6	0,45	53	83,65	71,13	15
Coil-7	0,45	80	86,24	72,37	16
Coil-8	0,45	106	86,77	75,13	13
Coil-9	0,45	133	87,75	76,31	13
Coil-10	0,90	26	82,07	70,14	15
Coil-11	0,90	40	86,24	77,60	10
Coil-12	0,90	53	86,77	80,10	8
Coil-13	0,90	66	87,09	81,61	6

The dataset comprises thirteen coils wound using three distinct wire diameters—0.20 mm, 0.45 mm, and 0.90 mm—and a varying number of turns. Each coil's theoretical and measured fill factor was calculated and compared, enabling an assessment of the accuracy and consistency of the system under diverse physical conditions.

The experimental winding results, in general, indicate that as the wire diameter and the number of turns increase, the measured fill factor (FF) values correspondingly increase, while the error rate between

theoretical and experimental values tends to decrease. This trend can be attributed to the greater structural stability and dimensional predictability of thicker wires.

A consistent trend is observed across all samples: as the wire diameter increases, the relative error between theoretical and measured fill factor values decreases. For coils wound with 0.20 mm wires, the theoretical fill factor ranged from 84.18% to 88.41%, while measured values were lower, between 72.22% and 77.41%. The relative error for this group of fine wires was observed to vary between 12% and 14%, averaging approximately 13.2%. These discrepancies are primarily attributed to the mechanical sensitivity of fine wires to process-induced variations. The high elasticity and high deformability [17] of thin wires make them more susceptible to deformation under tension, resulting in inconsistent layer formation and localized packing inefficiencies.

Moreover, minor inaccuracies in wire guidance or feed angle—which may not significantly affect thicker wires—tend to cause substantial deviations in the winding pattern when using thinner conductors. The absence of a closed-loop tension control mechanism exacerbates this issue, as fluctuations in reel torque and tension during winding cannot be actively corrected. This behavior is consistent with the findings reported by [18], who emphasized that precise tension control is crucial for maintaining constant wire resistance in fine wire winding applications.

In the case of 0.45 mm wire samples, the theoretical fill factor varied from 83.65% to 87.75%, while measured values were recorded between 71.13% and 76.31%. Despite the increased structural stability offered by the medium-sized wire, relative errors remained in the range of 13% to 16%. Notably, coils with lower turn counts, such as Coil-6 (53 turns) and Coil-7 (80 turns), displayed higher relative errors (15% and 16%, respectively), suggesting that coils with fewer layers are more vulnerable to proportional error amplification. In these cases, even small inconsistencies in wire deposition have a more pronounced impact on the overall fill factor.

Conversely, samples with higher turn counts, such as Coil-8 (106 turns) and Coil-9 (133 turns), demonstrated better alignment between theoretical and measured values, exhibiting reduced error margins of 13%. This suggests that increasing the number of turns allows for statistical averaging of layer inconsistencies, enhancing overall stability. The findings support observations made by [19], who demonstrated that multilayer winding processes benefit from cumulative alignment effects that reduce deviation.

The most favorable results were obtained with the 0.90 mm wire samples. The theoretical fill factor values ranged from 82.07% to 87.09%, while measured results spanned from 70.14% to 81.61%. In this group, the relative error dropped significantly, reaching as low as 6% in Coil-13, which achieved a measured fill factor of 81.61% against a theoretical prediction of 87.09%. This level of precision represents the most successful outcome across all experimental trials. The improved performance can be attributed to several inherent advantages associated with larger wire diameters. Firstly, the increased stiffness and mass of the wire enhance its resistance to deformation and dynamic instability, promoting more uniform stacking. Secondly, coarse wires exhibit greater inertial stability during high-speed rotation and are less sensitive to

minor discrepancies in feed angle or guide alignment. These factors collectively contribute to a more predictable and repeatable winding behavior, even under open-loop control conditions.

Across all thirteen samples, the average theoretical fill factor was calculated as 86.26%, while the average measured value was 75.07%, yielding a global mean error of 12.9%. This performance is in line with expectations for open-loop systems that lack closed-loop feedback. Moreover, mechanical limitations, such as 15 μm lead screw backlash and manual wire tensioning, contributed to irregularities. To address these issues, future iterations should incorporate closed-loop tension control systems, such as dancer arms, hysteresis brakes, or load cells [18].

The results obtained here fall within this performance envelope, suggesting that the system is competitive with contemporary winding solutions in its class, especially considering its modular architecture and low-cost components.

From an engineering standpoint, the system demonstrates the strongest reliability and repeatability when used with wire diameters of 0.90 mm and turn counts exceeding 40. In these conditions, the layer stacking was observed to be consistent, and the winding height measurements closely matched theoretical predictions. The step matrix-based microstepping strategy ensured synchronized motion between rotational and translational axes, maintaining controlled feed and spacing during the winding process. The system's performance in these configurations approaches the theoretical fill factor limit of 90.7% for circular wires in orthocyclic packing, as defined by [20]. Although the current system employs a helical winding method rather than true orthocyclic nesting, the results demonstrate that high-density packing can be achieved under well-optimized conditions.

Despite the presence of a step matrix-based synchronized motion control, the absence of adaptive speed control or feedback mechanisms restricts the system's performance when operating under sensitive winding conditions. These limitations become particularly prominent in fine-wire applications, where deviations introduced in early layers propagate through subsequent turns and accumulate into significant dimensional errors. Integrating a closed-loop tension control subsystem, such as a dancer arm equipped with load cell feedback, would allow for dynamic adjustment of reel torque and feed rate. This enhancement would help stabilize winding force and minimize radial bulging or under-stacking of wire layers. Additionally, incorporating a vision-based wire diameter monitoring system could assist in verifying the consistency of the feed material and detecting irregularities during operation.

Despite these challenges, the current system's strengths—especially its synchronous control, standalone operability via LCD interface, and modular structure—make it well-suited for rapid prototyping, laboratory-scale experimentation, and small-batch coil manufacturing. Its cost-effectiveness and use of open-source hardware (e.g., Arduino Mega and RAMPS 1.4) position it as a viable alternative to commercial systems, particularly for small and medium-sized enterprises (SMEs) seeking to internalize coil production without the overhead of proprietary automation solutions.

In conclusion, the developed helical coil winding system demonstrated strong potential for producing high-quality windings, particularly in medium and coarse wire configurations. The experimental results

support the validity of the system's mechanical design and synchronization algorithm, while also highlighting areas for improvement—most notably, tension feedback integration and adaptive feed control. By implementing these enhancements, the system could not only expand its applicability to fine-wire coils but also improve fill factor accuracy across all wire diameters. These developments would further bridge the performance gap between open-loop and closed-loop winding architectures and enhance the system's relevance for both academic and industrial applications.

4. CONCLUSION

In this study, an automatic helical coil winding system was developed and experimentally validated through a series of sample windings using various wire diameters and turn counts. The system demonstrated strong reliability and consistency, particularly for medium to coarse wire configurations (≥ 0.45 mm), achieving an average fill factor error of approximately 12.9%. The experimental results confirmed the effectiveness of the system's synchronized step-matrix-based motion control in maintaining uniform wire stacking and minimizing dimensional deviations.

Notably, larger wire diameters exhibited superior winding accuracy due to their inherent structural stability and resistance to process-induced perturbations. Meanwhile, fine-wire applications revealed the system's limitations in open-loop control environments, highlighting the need for enhancements such as closed-loop tension feedback and adaptive feed control mechanisms.

Despite these challenges, the modular architecture, cost-effectiveness, and standalone operation capabilities of the system establish it as a competitive alternative for laboratory-scale prototyping and small-batch production. Future work will focus on integrating dynamic tension control and vision-based monitoring systems to further improve precision, reduce error propagation in fine-wire applications, and enhance overall system performance. By addressing these improvements, the system's applicability can be expanded, bringing its performance closer to commercial-grade winding solutions while maintaining accessibility for academic and industrial users alike.

REFERENCES

1. P. R. Lord ve M. H. Mohamed, *Weaving: Conversion of Yarn to Fabric*, Durham: Mellow Technical Library, 1982.
2. S. T. Peters, *Composite Filament Winding*, Ohio: ASM International, 2011.
3. L. Novakova-Marcincinova ve I. Kuric, «Basic and Advanced Materials for Fused Deposition Modeling Rapid Prototyping Technology,» *Manuf. and Ind. Eng.* cilt 1, no. 24-27, 2012.
4. J. Hagedorn, F. SELL-LE BLANC ve J. FLEISCHER, *Handbook of Coil Winding*, Berlin: Springer Berlin Heidelberg, 2018.
5. Y. Li, A. G. Webb, S. Saha, W. W. Brey, C. Zachariah ve A. S. Edison, «Comparison of the performance of round and rectangular wire in small solenoids for high-field NMR,» *Magnetic Resonance in Chemistry*, cilt 3, no. 44, pp. 255-262, 2006.
6. J. BÖNIG, B. Bickel, M. Spahr, C. Fischer ve J. Franke, «Simulation of orthocyclic windings using the linear winding technique.,» *5th International Electric Drives Production Conference (EDPC)*, pp. 1-6, 15 Eylül 2015.

7. W. E. ALLEN, «Solenoid operated valve.» USA Patent: 4,295,631, 20 Ekim 1981.
8. V. DEL, M. Robert, B. Poulin, M. E. F. Feeney ve P. T. Feghali, Transformer design principles: with applications to core-form power transformers., CRC press, 2001.
9. S. H. WONG, M. Kupnik, X. Zhuang ve D. Lin, «Evaluation of wafer bonded CMUTs with rectangular membranes featuring high fill factor,» IEEE transactions on ultrasonics, ferroelectrics, and frequency control, cilt 9, no. 55, pp. 2053-2065, 19 Eylül 2008.
10. D. J. Gingery, Build a Universal Coil Winding Machine, Rogersville: David J Gingery Publishing, 1991.
11. Arduino, «MEGA 2560 REV3,» 2019. [Çevrimiçi]. Available: <https://store.arduino.cc/usa/mega-2560-r3>.
12. Reprap, «Ramps 1.4,» 7 Mart 2019. [Çevrimiçi]. Available: https://reprap.org/wiki/RAMPS_1.4.
13. H. APAYDIN, Adım motorlarının karakteristikleri ve bilgisayar ile konum kontrolü uygulaması, 2006.
14. T. HOPKINS, «Stepper motor driving,» Application note, STMicroelectronics, 2012.
15. ARDUINO, «What is Arduino?,» Arduino LLC, 2015. [Çevrimiçi]. Available: <https://www.arduino.cc/en/Guide/Introduction>.
16. N. ÖZEL, Doğru akım motoru ve step motorun mikroişlemci yardımıyla senkronizasyonu ve bobin sarma makinesine uyarlanması, Zonguldak, 2006.
17. A. Komodromos, C. Löbbe and A. E. Tekkaya, "Development of forming and product properties of copper wire in a linear coil winding process," 2017 7th International Electric Drives Production Conference (EDPC), Würzburg, Germany, 2017, pp. 1-7, doi: 10.1109/EDPC.2017.8328143
18. Jie-Shiou Lu, Ming-Yang Cheng, Ke-Han Su, Mi-Chi Tsai, Wire tension control of an automatic motor winding machine—an iterative learning sliding mode control approach, Robotics and Computer-Integrated Manufacturing, Volume 50, 2018, Pages 50-62, ISSN 0736-5845
19. J. Luo, P. Cao, B. Yu, M. Zhang and W. Xu, "The Coil Auto-lifting System of Intelligent Winding Machine," 2021 4th International Conference on Robotics, Control and Automation Engineering (RCAE), Wuhan, China, 2021, pp. 246-250
20. Florian Sell-Le Blanc, Janna Hofmann, Rico Simmler, Juergen Fleischer, Coil winding process modelling with deformation based wire tension analysis, CIRP Annals, Volume 65, Issue 1, 2016, Pages 65-68, ISSN 0007-8506